

Leukemia & Lymphoma Society. M.-A.H. was supported by a postdoctoral fellowship from Association pour la Recherche sur le Cancer (FRANCE). D.A.B. is a recipient of an NIH training grant.

Competing interests statement

The authors declare that they have no competing financial interests.

Correspondence and requests for materials should be addressed to R.S. (e-mail: shiekhattar@wistar.upenn.edu).

Reverse engineering of the giant muscle protein titin

Hongbin Li*, Wolfgang A. Linke†, Andres F. Oberhauser*, Mariano Carrion-Vazquez*, Jason G. Kerkvliet*, Hui Lu‡, Piotr E. Marszalek* & Julio M. Fernandez*

* Department of Physiology and Biophysics, Mayo Foundation, Rochester, Minnesota 55905, USA

† Institute of Physiology and Pathophysiology, University of Heidelberg, D-69120 Heidelberg, Germany

‡ Donald Danforth Plant Science Center, St Louis, Missouri 63132, USA

Through the study of single molecules it has become possible to explain the function of many of the complex molecular assemblies found in cells^{1–5}. The protein titin provides muscle with its passive elasticity. Each titin molecule extends over half a sarcomere, and its extensibility has been studied both *in situ*^{6–10} and at the level of single molecules^{11–14}. These studies suggested that titin is not a simple entropic spring but has a complex structure-dependent elasticity. Here we use protein engineering and single-molecule atomic force microscopy¹⁵ to examine the mechanical components that form the elastic region of human cardiac titin^{16,17}. We show that when these mechanical elements are combined, they explain the macroscopic behaviour of titin in intact muscle⁶. Our studies show the functional reconstitution of a protein from the sum of its parts.

Individual titin molecules span both the A-band and I-band regions of muscle sarcomeres. The I-band part of titin has been identified as the region that is functionally elastic. We study the shortest titin isoform, the N2B isoform found in cardiac-muscle sarcomeres. The elastic I-band region of N2B-titin can be subdivided into four structurally distinct regions (Fig. 1): a proximal immunoglobulin region containing 15 tandem immunoglobulin-like (Ig) domains; a middle N2B segment that contains a 572-residue amino-acid sequence of unknown structure; a 186-amino-acid-long segment rich in proline (P), glutamate (E), valine (V) and lysine (K) residues, named the PEVK region; and a distal Ig region that contains 22 tandem Ig modules¹⁷. We use polyprotein engineering^{18,19} and single-molecule force spectroscopy to dissect the individual mechanical elements of the I-band of cardiac titin and reconstruct the elasticity of cardiac muscle. Polyproteins, when mechanically stretched by single-molecule atomic force microscopy (AFM) give distinctive mechanical fingerprints as their modules unfold sequentially (sawtooth patterns in the force–extension curve)¹⁸, and can be used to positively identify the mechanical features of a single molecule^{19–21} (Supplementary Information).

The top trace in Fig. 1a shows a typical sawtooth pattern measured by stretching a protein composed of eight modules from the proximal tandem Ig region, I4 to I11. The sawtooth pattern shows that all modules unfold in the range of 150–200 pN. However, there is a slight tendency for the first unfolding event to occur at a lower force than later unfolding events. In order

to examine this tendency, we plot the average value of all first unfolding peaks, second peaks, and so on (Fig. 1b, filled circles). A linear fit to the data (Fig. 1b, thin line through filled circles) showed only a weak hierarchy of 12 pN per force peak. Polyproteins constructed using modules I4 (I4₈) and I5 (I5₈) showed similar unfolding forces of 150–200 pN (Fig. 1b, open circles). Hence, it seems that the proximal tandem Ig region has modules of similar mechanical stability. We studied the I4 polyprotein in more detail following the AFM protocols of ref. 18, and measured an unfolding rate of $3 \times 10^{-3} \text{ s}^{-1}$ and a folding rate of 0.33 s^{-1} .

Similar experiments done with polyproteins from the distal Ig region revealed a very different picture. Stretching a protein composed of eight modules from the distal tandem Ig region, I27 to I34, showed a much broader range of unfolding forces, from ~150 pN up to 330 pN (Fig. 1a, bottom trace). As before, we plot the average value of all first unfolding peaks, second peaks, and so on (Fig. 1b, filled squares). A linear fit to the data (Fig. 1b, thin line through

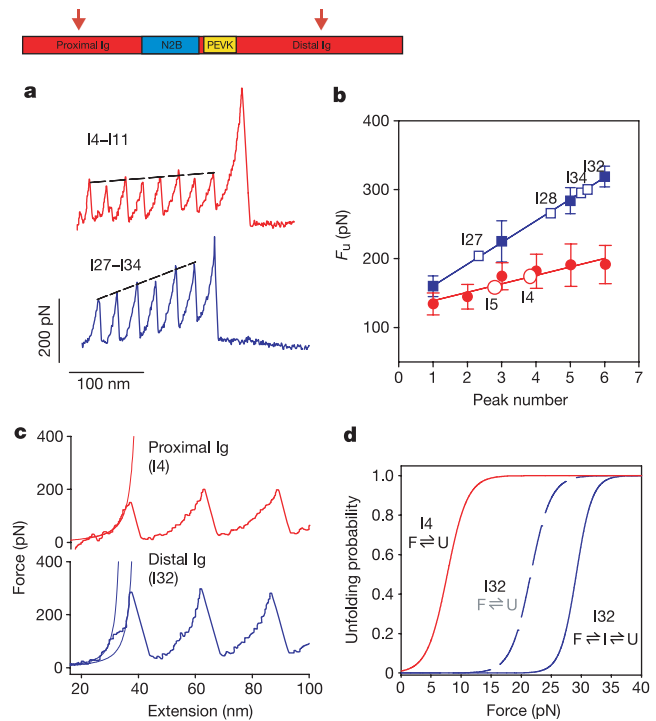


Figure 1 The proximal and distal tandem Ig regions of cardiac titin have different mechanical properties. Inset, the structurally distinct elements of I-band titin. The arrows point to the tandem Ig regions. **a**, Top trace: force–extension curve obtained from an engineered protein comprising domains I4 to I11 of the proximal tandem Ig region. Bottom trace: force–extension curve obtained from a protein comprising domains I27 to I34 of the distal tandem Ig region. **b**, Unfolding forces (F_u) measured for consecutive unfolding peaks (1–6) in AFM recordings of the I4–I11 protein (filled circles) and the I27–I34 protein (filled squares). Recordings obtained from polyproteins containing only I27, I28, I32, or I34 Ig domains (open squares; I27₈: $204 \pm 26 \text{ pN}$, $n = 266$; I28₈: $257 \pm 27 \text{ pN}$, $n = 245$; I34₈: $281 \pm 44 \text{ pN}$, $n = 32$; I32₈: $298 \pm 24 \text{ pN}$, $n = 132$) show a strong hierarchy. The stability of I4 and I5 polyproteins (open circles, I4₈ and I5₈; I4: $171 \pm 26 \text{ pN}$, $n = 136$; I5: $155 \pm 33 \text{ pN}$, $n = 196$) confirms the weak hierarchy of the proximal region. **c**, Top trace: force–extension relationship of an I4 polyprotein (I4₈). The initial part of the force trace, before the first unfolding peak, is well described by the WLC model (thin line). Bottom trace: force–extension relationship for an I32 polyprotein (I32₈) from the distal tandem Ig region of titin. In the initial rising phase of the force–extension curve, a prominent ‘hump’ appears, indicating the presence of an unfolding intermediate²⁴. **d**, Plot of the steady-state unfolding probability of the I4 and I32 modules as a function of force. I4 is calculated as a simple two-state unfolding system (solid red line). The I32 module is calculated both in the presence (solid blue line) and in the absence (dashed blue line) of the unfolding intermediate.

filled squares) gave a slope of 31.5 pN per force peak. These results indicate a mechanical hierarchy among these modules. In order to determine the mechanical stability of the individual modules and their ordering in the hierarchical unfolding, we constructed several polyproteins: I27₈, I28₈, I32₈ and I34₈. The average unfolding forces were found to be 204 pN for I27 (ref. 18), 257 pN for I28 (ref. 19), 298 ± 24 pN (*n* = 132) for I32 and 281 ± 44 pN (*n* = 32) for I34 (Fig. 1b, open squares). These results contrast with those for the proximal region where no obvious mechanical hierarchy was observed.

Several models of polymer elasticity have been developed to predict the mechanical behaviour of a polymer. As before, we use the worm-like chain (WLC)²² model to fit the force–extension curves of a polyprotein¹⁸. A close examination of the force–extension curve obtained from a proximal Ig module (I4₈, Fig. 1c) shows that the WLC model fits well the force–extension curve preceding each unfolding event (thin red line in Fig. 1c). The unfolding event that occurs is an all-or-none process that can be easily described by a two-state model of the type $F \rightleftharpoons U$ with rate constants for unfolding, $\alpha_u(F)$, and folding, $\beta_f(F)$, that are force dependent²³. Under a constant force *F*, the probability of unfolding is given by $P_u(F) = \alpha/(\alpha + \beta)$, which has a sigmoidal shape when plotted against the stretching force (Fig. 1d). The plot shows that for I4, $P_u(F) = 0.5$ at a force of 7.7 pN. This result is similar for I5, and is likely to be similar for the other modules of the proximal Ig region.

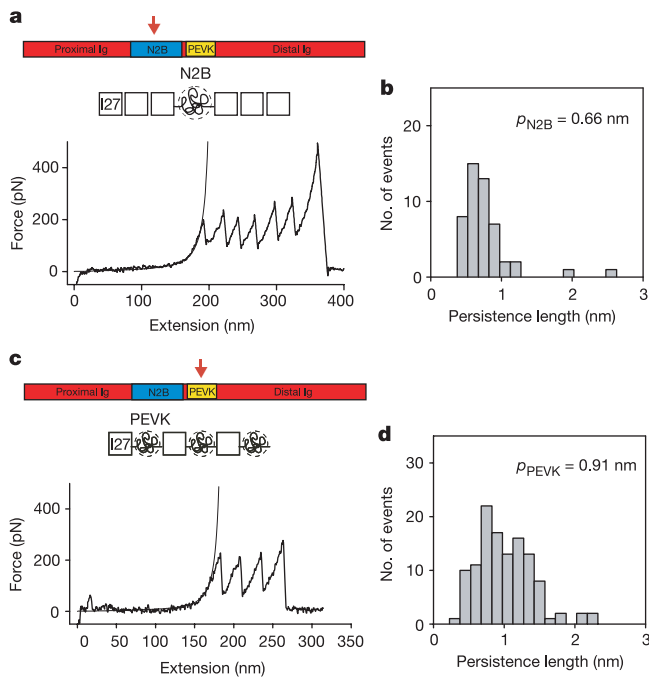


Figure 2 Single-molecule AFM measurements of the mechanical properties of the N2B and PEVK regions of titin. **a**, Top inset: the arrow points to the location of the N213 region in the I-band. Force–extension curve of a protein chimaera containing the cardiac N2B unique sequence flanked on either side by three I27 domains (I27₃-N2B-I27₃), bottom insert. A Levenberg–Marquardt fit of the WLC equation (thin line) to the force–extension curve before the first I27 unfolding event measured the contour length, L_c , and persistence length, ρ , of N2B. **b**, Frequency histogram of persistence-length values. A narrow distribution is found, centred at 0.66 nm. **c**, Top inset: the arrow points to the location of the PEVK region in the I-band. Force–extension curve of a protein chimaera containing human cardiac PEVK domains alternating with Ig I27 domains, (I27-PEVK)₃, bottom insert. As in **a**, we used Levenberg–Marquardt fits of the WLC equation to measure L_c and ρ of the PEVK region (thin line). **d**, Frequency histogram of persistence-length values measured for the PEVK domain. A relatively broad distribution is seen ($\rho = 0.4$ –2.5 nm; average value, 0.91 nm).

The WLC model does not fit the force–extension curve of the I32 polyprotein (Fig. 1c, bottom trace) because of a pronounced ‘hump’ that corresponds to an unfolding intermediate before full unfolding²⁴. We have observed a similar intermediate in all of the distal Ig modules tested, whereas we have not observed such an intermediate in the proximal domains. This unfolding intermediate may serve as a kinetic trap to stabilize the distal domains and protect them against unfolding. To illustrate this point, we first ignore the unfolding intermediate, and consider a simple two-state unfolding reaction with $P_u(F) = \alpha/(\alpha + \beta)$. The rate constants, α and β , are calculated from the peak unfolding forces and their dependence on the rate of stretching¹⁸, ignoring the unfolding intermediate. Figure 1d (dashed line) shows that $P_u(F) = 0.5$ at 21.6 pN for I32 in the absence of an unfolding intermediate. When the intermediate is considered, we use a simplified three-state model like $F \rightleftharpoons I \rightleftharpoons U$. Two sets of rate constants describe this model: α_u and β_u corresponding to the main unfolding reaction taken to occur between the intermediate and the unfolded state, and α_1 and β_1 describing the forward and backward rates of transition to the intermediate state. These last two rate constants were estimated from the data obtained for the intermediate unfolding state of the I27 module²⁴. The unfolding probability for the three-state model is given by:

$$P_u^I(F) = \frac{\alpha_1 \alpha_u}{\alpha_1 \alpha_u + \beta_1 \beta_u + \alpha_1 \beta_u} \quad (1)$$

The three-state unfolding probability is a sigmoidal function that is shifted to the right of that calculated without the unfolding intermediate. In this case, $P_u^I = 0.5$ at 29.2 pN. As the on-rate of the unfolding intermediate $\beta_1 = 100 \text{ s}^{-1}$ is much faster than the off-rate of the main unfolding event $\alpha_u = 0.01 \text{ s}^{-1}$, the module under force will not go directly to the unfolded state but rather go back to the folded state. Thus, this unfolding intermediate acts as an absorbing state (or buffering state) that kinetically prevents the module from unfolding. This difference in mechanical stability between distal and proximal Ig domains reflects the mechanical topology of these two classes of Ig modules (Supplementary Information).

In order to study the mechanical properties of the N2B segment, we constructed a polyprotein composed of a single N2B module

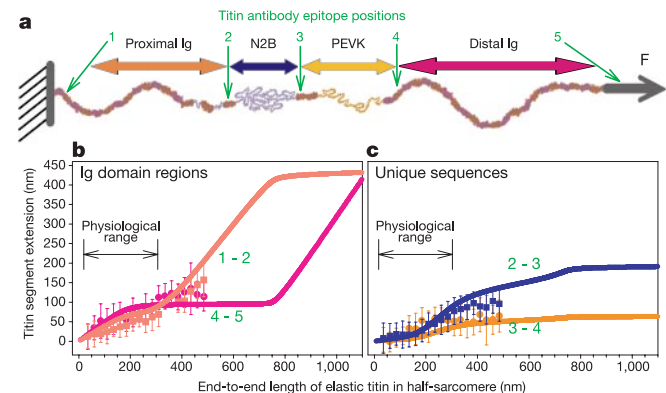


Figure 3 Single-molecule data explain the extensibility of the individual titin segments measured *in situ*. **a**, Schematic diagram showing the four main segments that contribute to the elasticity of titin in the half-sarcomere of cardiac muscle (horizontal arrows). Numbers 1–5 indicate the epitope positions of titin antibodies used to measure the extension of these segments *in situ*⁶. The epitopes move relative to one another when the muscle fibres are stretched. **b**, **c**, Extension of the individual titin segments plotted as a function of the end-to-end extension of I-band titin (symbols). The solid lines were calculated using equations (3)–(5), and the single-molecule data from Table 1. The numbers label the extension of the corresponding epitopes marking the proximal (1–2) and distal (4–5) Ig-domain regions, the N2B unique sequence (2–3) and the PEVK domain (3–4).

Table 1 Mechanical parameters describing the I-band region of human cardiac titin.

| | Unfolding rate α (s^{-1}) | Folding rate β (s^{-1}) | Persistence length p (nm) | Kuhn length l_k (nm) | Unfolding distance Δx_u (nm) | Folding distance Δx_f (nm) |
|-----------------------------------------------|-----------------------------------------|--------------------------------------|--------------------------------|--------------------------------|-----------------------------------------|---------------------------------------|
| Proximal Ig domains | $\alpha_u = 3.3 \times 10^{-3}$ | $\beta_u = 0.33$ | 10 (folded) 0.66 (unfolded) | 20 (folded) 1.32 (unfolded) | 0.25 | 2.2 |
| N2B unique sequence | — | — | 0.66 | 1.32 | — | — |
| PEVK segment | — | — | 0.91 | 1.82 | — | — |
| Distal Ig domains | $\alpha_u = 8 \times 10^{-5}$ | $\beta_u = 1.2$ | 10 (folded) 0.66 (unfolded) | 20 (folded) 1.32 (unfolded) | 0.25 | 2.2 |
| Unfolding intermediate (I), distal Ig domains | $\alpha_i = 1.0 \times 10^{-2}$ | $\beta_i = 10^2$ | — | — | 0.33 | 0.33 |

All values were obtained from single molecule force spectroscopy measurements, except for the persistence length of the folded Ig-domain regions, which was measured from EM images (Supplementary Information).

flanked on either side by three tandem I27 domains (I27₃-N2B-I27₃; Fig. 2a), where the I27 modules are used to create a mechanical fingerprint. We used single-molecule AFM to obtain force–extension curves from this polyprotein. We collected 48 recordings like the one in Fig. 2a showing a long initial region, without any unfolding peaks, followed by a sawtooth pattern with four to six consecutive unfolding events. The observed unfolding peaks of ~200 pN spaced by ~28 nm correspond to the characteristic fingerprint of the I27 module^{18–21}. If we observe at least four I27 unfolding events, then N2B must have been stretched when pulling this protein. Given that the extension of the segments of the protein will be hierarchical, from least stable to most stable^{19,20}, the long but featureless part of the trace preceding the sawtooth pattern must correspond to the extension of N2B. Then, extension of N2B occurs at low force and without significant energy barriers limiting its extensibility. This result suggests that the N2B segment has the mechanical properties of a random coil.

The WLC model (thin line, Fig. 2a) fits the force–extension curve of N2B and measures a contour length of 209 nm and a persistence length of $p = 0.74$ nm. Similar measurements made in 48 different recordings gave a distribution of persistence lengths that averaged $p_{N2B} = 0.66$ nm (Fig. 2b). We also measured an average contour length of 232 nm, which agrees well with the expected length of a 572-amino-acid-long polypeptide. We also constructed a polyprotein made of three repeats of the dimer PEVK-I27 (Fig. 2c, ref. 20). WLC fits to the force–extension curve of PEVK (thin line, Fig. 2c) measured an average contour length of 68 nm per PEVK segment²⁰. The persistence length of PEVK varied from 0.4 nm up to 2.5 nm with an average value of $p_{PEVK} = 0.91$ nm (Fig. 2d, ref. 20), suggesting that PEVK could show mechanical conformations that, while still corresponding to a random coil, had different flexibility.

The extensibility of each elastic segment of cardiac I-band titin has been measured in intact cardiac muscle fibres^{6,25}, by following the relative position of several sequence-specific titin antibodies (Fig. 3a). We reconstituted the extensibility of I-band titin by calculating the extension of each segment (proximal Ig, N2B, PEVK, distal Ig) at a given force, and repeating this calculation for a range of forces from 0 up to 40 pN. As all segments experience the same force at all times, the segments extend independently of each other and thus their contributions to the overall length are additive. The total end-to-end length of I-band titin, $x(F)_{I\text{-band}}$, is then calculated as the sum of the extension of all segments. The extensibility of a segment has two components: the entropic spring behaviour and module unfolding, if any^{11–13}.

The N2B and PEVK segments are entropic springs that do not show any unfolding events. These segments are simply modelled by the WLC approach, although with different persistence lengths (we use the average persistence length in each case; $p_{N2B} = 0.66$ nm and $p_{PEVK} = 0.91$ nm). However, the use of the WLC model in this reconstruction is inconvenient, because it gives the force that results from a given extension, $F(x)$, whereas we want to calculate the extension that results from an applied force. The freely jointed chain

model of polymer elasticity²⁶ is described by equation (2).

$$x_{FJC}(F) = L_c u\left(\frac{Fl_k}{k_B T}\right) \quad (2)$$

where L_c is the contour length, $u(Fl_k/k_B T)$ is the Langevin function (where K_B is the Boltzmann constant) and where the Kuhn length $l_k = 2p$ (ref. 22). We can now calculate the extension of these segments for a given force: $x(F)_{N2B}$ and $x(F)_{PEVK}$.

The extensibility of the proximal and distal tandem Ig domain segments, $x(F)_{proximal}$ and $x(F)_{distal}$, is also described by equation (2). However, in this case, L_c and l_k depend on module unfolding (Supplementary Information). Thus, the extension of the proximal Ig region under an applied force, $x(F)_{proximal}$, is fully described by the following three equations:

$$x(F)_{proximal} = L_c^{folded}(F) u\left(\frac{F l_k^{folded}}{k_B T}\right) + L_c^{unfolded}(F) u\left(\frac{F l_k^{unfolded}}{k_B T}\right) \quad (3)$$

$$L_c^{folded}(F) = N(1 - P_u(F))4.4 \quad (4)$$

$$L_c^{unfolded}(F) = N P_u(F)32.5 \quad (5)$$

where N is the total number of Ig modules in the segment and $P_u(F)$ is the probability of unfolding at a given force; equations (4) and (5) give lengths in units of nm. The extension of $x(F)_{distal}$ is calculated similarly but including a term for the contribution of the unfolding intermediate. We now calculate the total extension of I-band titin as:

$$x(F)_{I\text{-band}} = x(F)_{proximal} + x(F)_{N2B} + x(F)_{PEVK} + x(F)_{distal} \quad (6)$$

for forces ranging from 0 to 40 pN. This calculation creates a table of values relating $x(F)_{I\text{-band}}$ with $x(F)_{proximal}$, $x(F)_{N2B}$, $x(F)_{PEVK}$ and $x(F)_{distal}$. We can now compare the extensibility of each I-band titin segment with the extensibility measured *in situ*. The parameters used such as the values of persistence length and the unfolding/folding rate constants correspond to the experimentally determined values listed in Table 1. There are no free parameters in this computation.

Figure 3b compares the extensibility of the tandem Ig regions (proximal, orange line; distal, violet line), calculated with equation (6), with their *in situ* extensibility (symbols). The calculated extensibility of these segments agrees well with the myofibril data. The proximal domains extend first in a fully folded configuration. Unfolding of the proximal region becomes obvious at $x(F)_{I\text{-band}} > 300$ nm, whereas unfolding of the distal Ig region does not occur until much later at $x(F)_{I\text{-band}} > 800$ nm. Hence, the single-molecule data predict that in the physiological range ($0 < x(F)_{I\text{-band}} < 300$ nm) the distal Ig region will never unfold any of its modules whereas the proximal region may see a few of its modules unfold towards the high end of the physiological range. Figure 3c shows plots of $x(F)_{N2B}$ (blue line) and of $x(F)_{PEVK}$ (orange line) versus the end-to-end length of the I-band titin, $x(F)_{I\text{-band}}$. The figure shows

that the calculated extension of these segments fits those measured *in situ* (symbols).

Figure 4 plots the relationship between force and the end-to-end length of I-band titin, $x(F)_{I\text{-band}}$ calculated from equation (6) (solid red line). We compare this calculation with the passive force versus sarcomere length relationship of an intact cardiac myofibril⁶ measured under quasi-steady-state conditions (no viscous or viscoelastic forces present)^{6,27}. The filled symbols in Fig. 4 correspond to single cardiac myofibril data scaled by the number of titin molecules per cross-sectional area of muscle (assumed to be 6×10^9 titin molecules per mm^2)²⁸. The figure shows that the force–extension relationship calculated from the single-molecule AFM data faithfully predicts the force–extension relationship measured in intact myofibrils. So by scaling the single-molecule data, it is possible to reproduce the passive elasticity of an intact myofibril. A similar reconstruction can also be done by numerically inverting the WLC model of polymer elasticity (Supplementary Information).

The physiological range of sarcomere lengths for a cardiac myofibril is 1.8–2.4 μm (ref. 29), corresponding to an extension range of 0–300 nm for I-band titin. The single-molecule data show that at an extension of 300 nm, the force reaches ~ 4 pN per I-band titin molecule. This force is about the same as that generated by a single myosin molecule⁴. At this force, the unfolding probability of the proximal tandem Ig region is low, $P_u = 0.1$. By contrast, the unfolding probability of the distal region is six orders of magnitude smaller. These results show that towards the end of the physiological range, unfolding of a few proximal Ig domains is possible whereas the distal domains always remain folded. If the unfolding probability of the proximal and distal Ig regions was zero, we would observe a purely entropic force–extension relationship (Fig. 4, black line). A purely entropic mechanism explains most of the extensibility of I-band titin in the physiological range, however, it departs significantly at higher extensions. These results suggest that unfolding of the proximal tandem Ig region may serve as a buffer to protect cardiac sarcomeres from developing damaging high forces. This becomes clear if we compare the effects of an over-extension to 450 nm. I-band titin will respond by unfolding several proximal Ig domains, limiting the force to ~ 7 pN. By contrast, if unfolding were

not possible, the force developed would exceed 40 pN per molecule, probably damaging sarcomeric structures. □

Methods

Protein engineering

All constructs were from human cardiac titin^{16,17}. Titin modules I4–I11, I4, I5, PEVK and N2B were cloned by polymerase chain reaction with reverse transcription (RT–PCR) from human heart poly(A)⁺ mRNA (Clontech) using the ThermoScript System (Gibco–BRL). Polyproteins I27₈, I28₈, I32₈, I34₈, I4₈, I5₈ and I27₃–N2B–I27₃ were constructed using a previously described method based on the identity of the sticky ends generated by *Bam*HI and *Bgl*II restriction enzymes^{18,19}, and then subcloned into pQE 80L (I4₈ and I5₈) or pQE 30 (I27₈, I28₈, I32₈, I34₈, I27₃–N2B–I27₃), (Qiagen). I27₁₂ was constructed using a non-palindromic *Ava*I restriction site (CTCGGG), as previously described¹⁸. (I27–PEVK)₃ was constructed using a similar method after *Eco*RI ligation of the two domains. (I27–PEVK)₃ and I4–I11 were cloned into pET–Ava I (ref. 18) while I27–I34 was cloned in pET 9d (ref. 11). The I27–I34 plasmid was a gift from M. Gautel¹¹. This protein has five changes to the sequence published for titin¹⁷: Thr 42 is replaced by Ala, and Ala 78 is replaced by Thr in the I27 module, Ala 53 is replaced by Thr in the I30 module, there is a deletion that includes the last two codons of I32 and 87 codons of the I33 domain^{18,30}, and a deletion of the Glu 89 codon of I34. The cloning strain was SURE-2 (Stratagene). The expression strains used were BL21 (DE3) (I27–I34), BLR (DE3) (I4₈, I5₈, (I27–PEVK)₃), BL21 (DE3) CodonPlus (I4–I11), SURE-2 (I27₈, I27₃–N2B–I27₃), and M15 (I28₈, I32₈, I34₈). Purification of recombinant proteins, from the soluble fraction of the bacterial lysate, was done by Ni²⁺-affinity chromatography in all the cases but for I4–I11, in which Co²⁺-affinity purification was used (Clontech). In the case of (I27–PEVK)₃ an additional size-exclusion fast performance liquid chromatography (FPLC) step was used. Proteins were kept at 4 °C in PBS with 5 mM dithiothreitol (DTT) and 0.2 mM EDTA, except for I27₈, I28₈, I32₈, I34₈, which were kept in 100 mM imidazole (pH 6.0). All the constructs used in this study have a His-tag at the amino terminus for affinity purification and two Cys residues at the carboxy terminus to promote covalent attachment of the protein to the gold-coated substrate.

AFM

Protein samples (3–10 μl , at a concentration of 10–100 $\mu\text{g ml}^{-1}$) were deposited onto freshly evaporated gold coverslips to allow the protein to adsorb onto the gold surface. Force–extension measurements were then carried out in PBS saline buffer (137 mM sodium chloride, 2.7 mM potassium chloride and 10 mM phosphate buffer, pH 7.4). The cantilevers are standard Si₃N₄ cantilevers from either Digital Instruments (with a typical spring constant of 100 mN m^{-1}) or TM Microscopes (with a typical spring constant of 12 mN m^{-1}). Every cantilever was calibrated in solution before use.

In situ recording of titin extensibility and force generation

The extensibility of the various I-band titin segments of rabbit cardiac myofibrils were measured using immunoelectron/immunofluorescence microscopy with a set of titin-specific antibodies⁶. Rabbit cardiac muscle expresses almost exclusively the N2B form¹⁶. Here, the technical names of the antibodies (T12, I17, I18, I20/22, MIR) were replaced for simplicity by consecutive numbers 1 to 5, with 1 being closest to the Z-disk and 5 being located at the A-band/I-band junction (Fig. 3). For each antibody type, the epitope-mobility data obtained over a range of sarcomere lengths (SLs) from 1.8 to 2.8 μm were pooled in SL bins of 50 nm. For each SL bin, the extension of a given titin segment was measured as the distance flanked by two nearest antibody epitopes: proximal Ig region, epitope 1 to epitope 2; N2B, 2 to 3; PEVK, 3 to 4; and distal Ig region, 4 to 5. The epitopes 3 and 4, which measure the extension of PEVK segment, include four additional Ig domains, hence the PEVK extension data were offset by 20 nm. Titin segment extension was then plotted against extension of the entire elastic titin in a half-sarcomere, $x(F)_{I\text{-band}}$, obtained as $x(F)_{I\text{-band}} = (\text{SL} - 1.8 \mu\text{m})/2$, to account for the functionally stiff titin in the sarcomere (1.6 μm in A-band, $2 \times 0.1 \mu\text{m}$ adjacent to Z-disk). The corresponding stretching force, F , was determined from mechanical recordings of the passive tension of isolated rabbit cardiac myofibrils^{6,27} immersed in a buffer solution (6 mM magnesium methanesulphonate, 5 mM dipotassium methanesulphonate, 4 mM Na₂ATP, 15 mM EGTA, with a total ionic strength of 200 mM adjusted with KOH in a 3-N-morpholino-propanesulphonic acid buffer, pH 7.1, 40 $\mu\text{g leupeptin ml}^{-1}$). Experimental protocols have been described²⁷. Passive force was recorded under quasi-steady-state conditions, that is, two to three minutes following a stretch to a new sarcomere length, to exclude viscous and viscoelastic force components that decay during stress relaxation.

Received 5 November 2001; accepted 14 June 2002; doi:10.1038/nature00938.

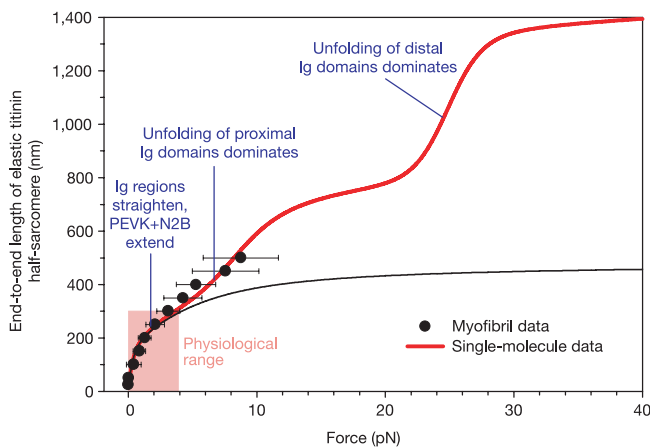


Figure 4 Single-molecule data predict the force–extension curve of cardiac muscle. The red line plots the calculated (equation (6)) end-to-end length of I-band titin versus a stretching force. The black line also plots equation (6), but in this case the unfolding probability of both the proximal and distal tandem Ig regions was set to zero. The symbols plot force–extension measurements from non-activated rabbit cardiac myofibrils. The values of the measured force were scaled to a single molecule assuming 6×10^9 titin molecules per mm^2 of cross-sectional area. The data show that the single-molecule data fully explain the force–extension relationship within and beyond the physiological range (coloured box).

1. Sigworth, F. J. & Neher, E. Single Na⁺ channel currents observed in cultured rat muscle cells. *Nature* **287**, 447–449 (1980).
2. Bustamante, C., Smith, S. B., Liphardt, J. & Smith, D. Single-molecule studies of DNA mechanics. *Curr. Opin. Struct. Biol.* **10**, 279–285 (2000).
3. Smith, D. E. *et al.* The bacteriophage $\phi 29$ portal motor can package DNA against a large internal force. *Nature* **413**, 748–752 (2001).
4. Finer, J. T., Simmons, R. M. & Spudis, J. A. Single myosin molecule mechanics: piconewton forces and nanometre steps. *Nature* **368**, 113–119 (1994).
5. Lu, H. & Schulten, K. Steered molecular dynamics simulations of force-induced protein domain unfolding. *Proteins Struct. Funct. Genet.* **35**, 453–463 (1999).
6. Linke, W. A. *et al.* I-band titin in cardiac muscle is a three-element molecular spring and is critical for maintaining thin filament structure. *J. Cell Biol.* **146**, 631–644 (1999).
7. Maruyama, K. Connectin/titin, giant elastic protein of muscle. *FASEB J.* **11**, 341–345 (1997).

8. Wang, K. Titin/connectin and nebulin: giant protein rulers of muscle structure and function. *Adv. Biophys.* **33**, 123–134 (1996).
9. Gregorio, C. C., Granzier, H., Sorimachi, H. & Labeit, S. Muscle assembly: a titanic achievement? *Curr. Opin. Cell Biol.* **11**, 18–25 (1999).
10. Trinick, J. & Tskhovrebova, L. Titin: a molecular control freak. *Trends Cell Biol.* **9**, 377–380 (1999).
11. Rief, M., Gautel, M., Oesterhelt, F., Fernandez, J. M. & Gaub, H. E. Reversible unfolding of individual immunoglobulin domains by AFM. *Science* **276**, 1109–1112 (1997).
12. Kellermayer, M., Smith, S., Granzier, H. & Bustamante, C. Folding–unfolding transitions in single titin molecules characterized with laser tweezers. *Science* **276**, 1112–1116 (1997).
13. Tskhovrebova, L., Trinick, J., Sleep, J. A. & Simmons, R. M. Elasticity and unfolding of single molecules of the giant muscle protein titin. *Nature* **387**, 308–312 (1997).
14. Tskhovrebova, L. & Trinick, J. Direct visualization of extensibility in isolated titin molecules. *J. Mol. Biol.* **265**, 100–106 (1997).
15. Fisher, T. E., Marszalek, P. E. & Fernandez, J. M. Stretching single molecules into novel conformations using the atomic force microscope. *Nature Struct. Biol.* **7**, 719–724 (2000).
16. Freiburg, A. *et al.* Series of exon-skipping events in the elastic spring region of titin as the structural basis for myofibrillar elastic diversity. *Circ. Res.* **86**, 1114–1121 (2000).
17. Labeit, S. & Kolmerer, B. Titins, giant proteins in charge of muscle ultrastructure and elasticity. *Science* **270**, 293–296 (1995).
18. Carrion-Vazquez, M. *et al.* Mechanical and chemical unfolding of a single protein: a comparison. *Proc. Natl Acad. Sci. USA* **96**, 3694–3699 (1999).
19. Li, H. B., Oberhauser, A. F., Fowler, S. B., Clarke, J. & Fernandez, J. M. Atomic force microscopy reveals the mechanical design of a modular protein. *Proc. Natl Acad. Sci. USA* **97**, 6527–6531 (2000).
20. Li, H. B. *et al.* Multiple conformations of PEVK proteins detected by single-molecule techniques. *Proc. Natl Acad. Sci. USA* **98**, 10682–10686 (2001).
21. Best, R. B., Li, B., Steward, A., Daggett, V. & Clarke, J. Can non-mechanical proteins withstand force? Stretching barnase by atomic force microscopy and molecular dynamics simulation. *Biophys. J.* **81**, 2344–2356 (2001).
22. Marko, J. F. & Siggia, E. D. Stretching DNA. *Macromolecules* **28**, 8759–8770 (1995).
23. Bell, G. I. Models for the specific adhesion of cells to cells. *Science* **200**, 618–627 (1978).
24. Marszalek, P. E. *et al.* Mechanical unfolding intermediates in titin modules. *Nature* **402**, 100–103 (1999).
25. Trombitas, K., Freiburg, A., Centner, T., Labeit, S. & Granzier, H. Molecular dissection of N2B cardiac titin's extensibility. *Biophys. J.* **77**, 3189–3196 (1999).
26. Bueche, F. *Physical Properties of Polymers* 37 (Interscience, New York, 1962).
27. Linke, W. A. *et al.* Towards a molecular understanding of the elasticity of titin. *J. Mol. Biol.* **261**, 62–71 (1996).
28. Higuchi, H., Nakauchi, Y., Maruyama, K. & Fujime, S. Characterization of beta-connectin (titin 2) from striated muscle by dynamic light scattering. *Biophys. J.* **65**, 1906–1915 (1993).
29. Allen, D. G. & Kentish, J. C. The cellular basis of the length-tension relation in cardiac muscle. *J. Mol. Cell Cardiol.* **17**, 821–840 (1985).
30. Scott, K. A., Steward, A., Fowler, S. B. & Clarke, J. Titin; a multidomain protein that behaves as the sum of its parts. *J. Mol. Biol.* **315**, 819–829 (2002).

Supplementary Information accompanies the paper on *Nature's* website (<http://www.nature.com/nature>).

Acknowledgements

We thank H. Erickson for the electron microscope pictures of I27 polyproteins. W.A.L. thanks the German Research Foundation for a Heisenberg fellowship. This work was supported by the National Institutes of Health (J.M.F.)

Competing interests statement

The authors declare that they have no competing financial interests.

Correspondence and requests for materials should be addressed to J.M.F. (e-mail: jfernandez@columbia.edu).